Pushdown Tests on Masonry Infilled Frames for Assessment of Building Robustness

Francisco B. Xavier[1]; Lorenzo Macorini[2]; Bassam A. Izzuddin, M.ASCE[3]; Corrado Chisari[4]; Natalino Gattesco[5]; Salvatore Noe[6]; and Claudio Amadio, M.ASCE[7]

Abstract: The research presented in this paper addresses the influence of nonstructural masonry infill on the resistance of multistory buildings to progressive collapse under sudden column loss scenarios. In particular, the structural response of infilled frames in peripheral bays is investigated within the scope of a design-oriented robustness assessment framework previously developed at Imperial College London. This allows due consideration of structural redundancy, ductility, strength, dynamic effects, and energy absorption capabilities in a unified manner. The realistic contribution of masonry panels toward collapse arrest is examined considering the results from full-scale laboratory tests performed on different two-bay frames with brick-masonry infill subjected to incremental pushdown deformation, capturing the dominant deformation mode found following removal of an edge column. In these physical tests, it is observed that the failure mechanisms and damage patterns displayed by the infill panels under pushdown deformation are similar to those activated by lateral pushover loading. Clear evidence of diagonal cracking and shear sliding, eventually culminating in crushing of the compressed corners, is noted. Different infill configurations are tested, including central openings and an initial gap between masonry and frame elements. Overall, a global stable response is observed even in the presence of severe damage in the masonry panels, delivering a monotonic supply of energy absorption with increasing downward displacement. The outcome from this experimental research provides mechanically sound and quantifiable evidence that nonstructural masonry infill panels in peripheral frames offer a reliable and efficient source of enhanced robustness under column loss events. Because of the widespread application of masonry infill panels, this is believed to be particularly relevant within the context of retrofitting operations for robustness enhancement of existing structures, as a result of the growing demand for upgraded resilience of urban infrastructure. Similarly, due account for masonry infill subject to proper quality control during the construction process is recommended for rational robustness design of new buildings. **DOI: 10.1061/(ASCE)ST.1943-541X.0001777.**

Author keywords: Masonry infill; Experimental test; Progressive collapse; Robustness assessment; Alternate load path; Concrete and masonry structures.

Introduction

According to standard practice in structural design, unreinforced masonry (URM) infill panels are often assumed as nonstructural components, meaning that their contribution is not quantified when assessing the integrity of the primary structure. However, because of their inherent in-plane stiffness and strength, infill walls may substantially influence the mechanical characteristics of framed buildings (Negro and Colombo 1997). This is particularly true under seismic actions, as inspections of damage patterns after past earthquakes have clearly revealed that the influence of URM panels may be in some cases beneficial while in others detrimental (Mosalam and Günay 2015). Depending on many factors ranging from the relative frame-infill mechanical properties to the geometrical layout and infill distribution, masonry panels may either enhance building resistance or trigger unexpected brittle failure.

Conversely, with regards to local damage events, the contribution of masonry infill is typically seen as beneficial, as pointed out by a recent survey of research on building robustness (Arup 2011), and as mentioned in Cormie et al. (2009) and Smith et al. (2010) for the specific case of resistance to blast loading. Such enhanced performance is intuitively justified by the assumption that on severe damage or removal of primary structural elements, masonry panels enable the activation of alternative paths for gravity loads, acting de facto as a composite system with the surrounding frame and floors. In this way, it might be argued that URM infill effectively introduces a substantial strength reserve under extreme localized hazards. This is significant as current trends in structural design are increasingly concerned with the detailing of components to enhance building response under accidental scenarios, with particular emphasis on the influence of localized hazardous events on the global behavior (Arup 2011). This is reflected in design codes such as EN 1991-1-7 (CEN 2006) that impose special robustness requirements on new structures, leading to increased costs because of upgraded detailing. Similarly, concern exists on the retrofitting of

[1]Former Ph.D. Candidate, Dept. of Civil and Environmental Engineering, Imperial College London, South Kensington Campus, London SW7 2AZ, U.K. E-mail: francisco.xavier11@alumni.imperial.ac.uk

[2]Senior Lecturer, Dept. of Civil and Environmental Engineering, Imperial College London, South Kensington Campus, London SW7 2AZ, U.K. (corresponding author). E-mail: l.macorini@imperial.ac.uk

[3]Professor of Computational Structural Mechanics, Dept. of Civil and Environmental Engineering, Imperial College London, South Kensington Campus, London SW7 2AZ, U.K. E-mail: b.izzuddin@imperial.ac.uk

[4]Postdoctoral Research Assistant, Dept. of Engineering and Architecture, Univ. of Trieste, 34127 Trieste, Italy.

[5]Associate Professor, Dept. of Engineering and Architecture, Univ. of Trieste, 34127 Trieste, Italy.

[6]Professor of Structural Engineering, Dept. of Engineering and Architecture, Univ. of Trieste, 34127 Trieste, Italy.

[7]Associate Professor, Dept. of Engineering and Architecture, Univ. of Trieste, 34127 Trieste, Italy.

Note. This manuscript was submitted on January 23, 2016; approved on December 15, 2016; published online on May 11, 2017. Discussion period open until October 11, 2017; separate discussions must be submitted for individual papers. This paper is part of the ***Journal of Structural Engineering***, © ASCE, ISSN 0733-9445.

existing structures to resist progressive collapse, as demonstrated in recent application cases by Adaros and Smilowitz (2014) and Naderi et al. (2015). For this reason, exploring the possible contribution arising from URM panels, which are often used in framed buildings, constitutes a rational and convenient way to secure the desired degree of robustness in both new and existing structures.

Unfortunately, the extent to which URM panels are actually responsible for this performance enhancement is not easily demonstrated from a quantitative stand point. Furthermore, under such extreme scenarios, it is widely acknowledged that other mechanisms play a fundamental role in the collapse arrest process, including three-dimensional load redistribution, floor membrane effects, beam arching, and catenary action (Izzuddin et al. 2008; Vlassis et al. 2008; Arup 2011; Li and Qian 2014). Consequently, bearing in mind the potential benefits of properly incorporating URM infill in robustness assessments, a comprehensive research project was developed to address this topic, combining advanced numerical analysis and with experimental tests within the scope of a progressive collapse assessment framework (Xavier 2015). This paper details the experimental work undertaken within this project, presents the associated experimental results, and provides an analysis of these results focusing on the significance of infill panels for structural robustness. In particular, the objectives of the experimental work described in this paper are to (1) quantify the pushdown capacity of confined infill panels in terms of vertical force and energy absorption, and (2) qualitatively assess the incremental damage in the masonry panels in order to confirm the analogy with the widely investigated lateral pushover response in earthquake engineering.

A summary of the progressive collapse assessment framework of Izzuddin et al. (2008) is first presented, as it provides the theoretical basis for the interpretation of the experimental outcomes with respect to sudden column loss events. Subsequently, the experimental program is described, and the results of the full-scale pushdown tests are presented. Finally, the responses of the real-scale specimens are analyzed within the energy-based framework (Izzuddin et al. 2008), considering also the results of numerical simulations conducted using simple numerical descriptions for masonry infill. The results obtained provide a meaningful measure of the dynamic response of infilled frames under column loss events.

Ductility-Centered Robustness Assessment Framework

The approach introduced by Izzuddin et al. (2008) for robustness assessment under sudden column loss is employed to establish a *robustness limit state* beyond which local damage develops into disproportionate global collapse. This method hinges on the fact that under column loss scenarios the global response is governed by a dominant downward deformation mode [Fig. 1(a)]. In this way, it is possible to idealize the affected part of the building structure as a generalized single-degree-of-freedom (SDOF) system, where all relevant mechanical features are inherently captured by increasing the complexity of the employed numerical descriptions. As in any SDOF representation, the generalized system is equivalent to the real structure in terms of deformation and kinetic energy. This allows the use of simple energy balance principles to obtain the maximum dynamic deformation due to column loss considering only the nonlinear static response. This represents one of the primary practical advantages of this method, which bypasses the need for cumbersome direct nonlinear dynamic computations.

The method is applied in three main steps (Izzuddin et al. 2008):

1. Performing nonlinear static pushdown analysis on the relevant structure without the affected column. A curve relating generalized load and displacement of the idealized SDOF system is obtained (where the relevant structural features are possibly captured by increasing the model complexity). This concept is better illustrated with the aid of Fig. 1, where a possible curve arising from the static pushdown response of the hypothetical system in Fig. 1(a) could be represented by the solid line in the left and central graphs in Fig. 1(b). In the present paper, the real-scale tests are employed to obtain this realistic pushdown curve for the URM infilled frames;
2. Determining the simplified dynamic response through the application of energy conservation principles given the generalized nonlinear static curve. This process is sketched in Fig. 1(b), where the maximum dynamic displacement $u_{d,i}$ occurs when the strain energy absorbed by the structure equals the work done by the gravity load $\lambda_i P_0$. The nonlinear static curve is transformed into a pseudostatic curve by performing the energy balance for different levels of gravity load, which relates the different levels of applied gravity load $\lambda_i P_0$ to the maximum dynamic

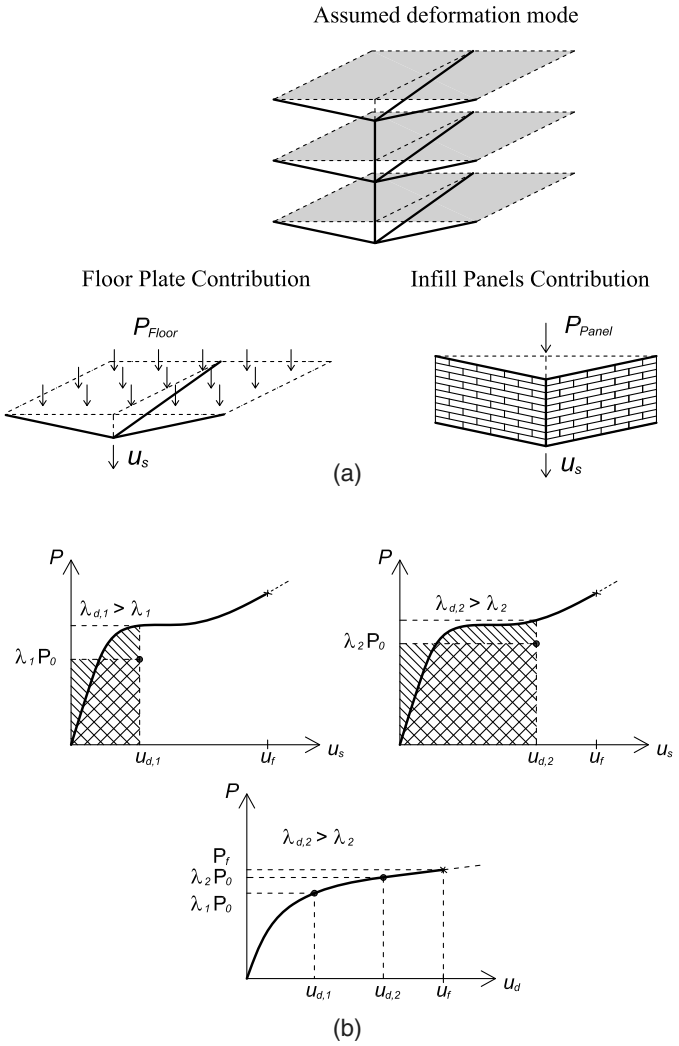

Fig. 1. (a) Assumed dominant pushdown deformation mode accounting for the floor and infill contributions; (b) simplified dynamic procedure to obtain pseudostatic response [(a and b) adapted from *Engineering Structures*, 30(5), B. A. Izzuddin, A. G. Vlassis, A. Y. Elghazouli, and D. A. Nethercot, "Progressive collapse of multi-storey buildings due to sudden column loss—Part I: Simplified assessment framework," pp. 1308–1318, Copyright (2008), with permission from Elsevier]

displacement at column loss position $u_{d,i}$. Formally, the pseudostatic resistance **P** is given by

$$\mathbf{P} = \frac{1}{u_d}\int_0^{u_d} P du \tag{1}$$

where P = nonlinear static resistance; and

3. Conducting ductility assessment by direct comparison between ductility supply and demand. This provides a single rational measure of robustness, where the influence of redundancy, ductility, dynamic effects, and energy absorption are combined leading to a ductility-centered procedure (Izzuddin et al. 2008; Izzuddin and Nethercot 2009; Izzuddin 2010).

As a matter of reference, the previously listed procedure has been employed on preliminary studies focused on influence of URM infill under column loss where the masonry panels were represented by simplified struts (Farazman et al. 2013) and advanced FE mesoscale models (Xavier et al. 2015). In both instances, considerable enhancement of pseudostatic capacity was noted where the early stage frame-infill interaction is particularly relevant, as revealed by the sophisticated modeling strategy. Despite the encouraging results cited earlier, because of the inherent complexities associated with the highly nonlinear response of URM assemblages, real-scale physical evidence is required to corroborate such initial numerical findings. Of course, this constitutes a crucial motivation factor leading to the tests presented in this paper. Before proceeding with the experimental results, it must be stressed that despite the fact that the floor slabs are not explicitly accounted for in the pushdown tests, such contribution might be added a posteriori in accordance to the dominant downward deformation mode [Fig. 1(a)]; see Izzuddin et al. (2008) for theoretical justification. In fact, the advantage of this decomposition is the possibility to compare the relative importance of each component at different levels of ductility demand. Nonetheless, in this work attention is devoted to the individual pushdown response of peripheral frames with URM infill in terms of strength, ductility, and failure modes. A more complete discussion of the relative influence of URM infill and the floor system response can be found elsewhere (Xavier 2015).

Experimental Program Overview

Test Apparatus Configuration

As opposed to standard experimental programs on infilled frames, in the experimental work presented in this paper there is no intention of proceeding with comparative assessments between infilled and bare frame performances. Instead, the objective is to quantify the pushdown capacity of confined masonry panels under pushdown deformation and identify the typical response mechanisms. For this reason, the adopted steel structure does not correspond to a typical building configuration [Fig. 2(a)], meaning that the bare response is of no relevant interest if considered in isolation. In this respect, the structural frame was designed with the aim of displaying a quasi-mechanism response when subjected to the applied vertical load, thus allowing the resistance to the pushdown deformation to be transferred to the confined masonry panels. Of course, no perfect vertical mechanism was practical to implement. Thus the adopted bolted connections [Fig. 2(b)] deliver a compromise solution providing low flexural strength and stiffness but significant shear and axial resistance, while allowing the development of large rotations at the beam-column joints. Furthermore, all the steel

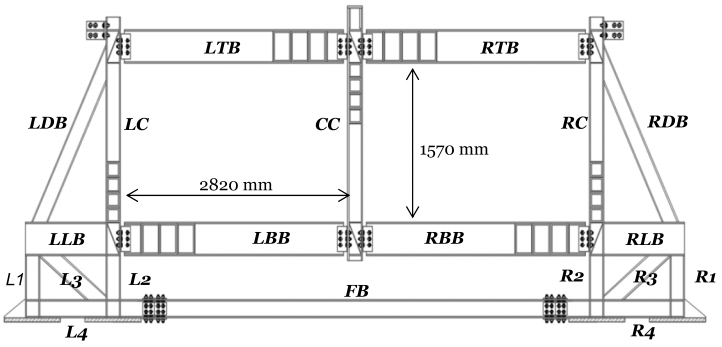

(a)

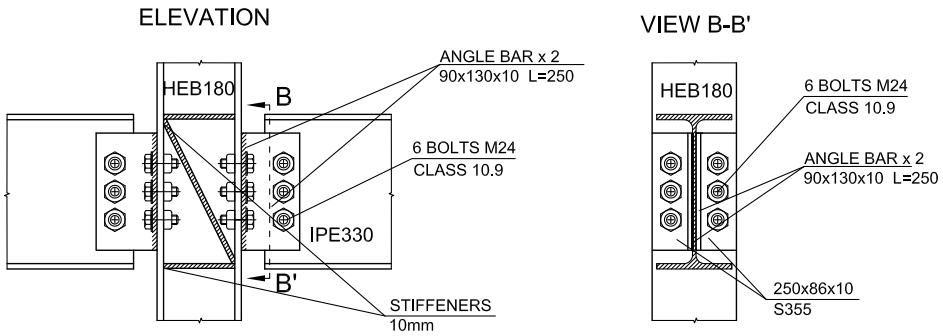

(b)

Fig. 2. (a) Elevation view of the bare steel frame and the lateral bracings; (b) adopted partial-depth beam-column connection detail

Table 1. Steel Sections for the Members of the Test Specimens (S355)

Type	Label	Profile
Beam	LTB, RTB, LBB, RBB	IPE 330
Column	LC, CC, RB	HEB 180
Bracing	LDB, RDB, L3, R3	HEB 180
Beam	FB, L4, R4	HEB 180
Column	L1, L2, R1, R2	HEB 180
Beam	LLB, RLB	IPE 330

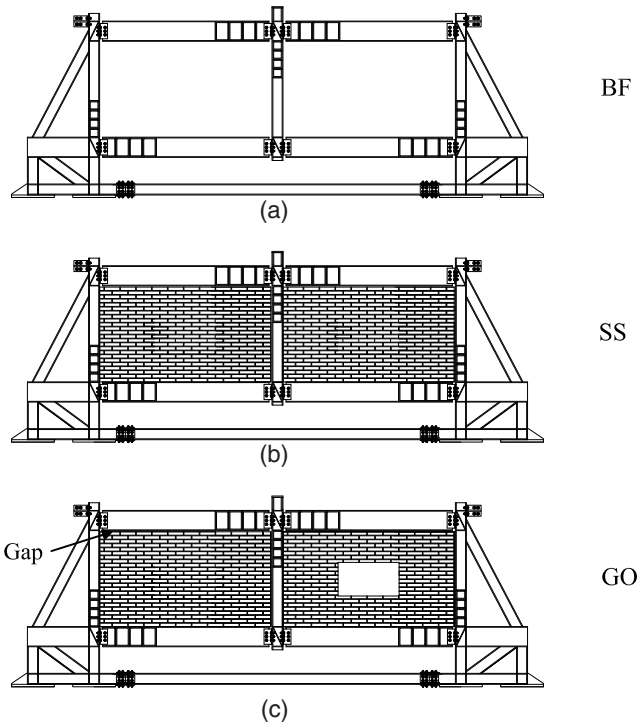

Fig. 3. Summary of experimental tests: (a) bare frame (BF); (b) symmetric solid panels (SS); (c) solid with gap and perforated panels (GO)

members were dimensioned to resist the applied loads remaining well within the elastic limit, thus enabling the use of the same frame components for different tests with only minimum damage in specific parts of the connections that can be easily substituted after each test. The employed steel sections are listed in Table 1, where the member's labeling is explicit in Fig. 2(a).

Description of Test Specimens

The tests (Fig. 3) are specifically intended to reproduce the response of a peripheral bay, i.e. edge beams and columns with the corresponding masonry infill as depicted in Fig. 1(a). The particular cases of corner and interior column losses are outside the scope of this paper.

The elevation and plan views of the steel specimen are shown in Figs. 2(a) and 4, respectively. The first infilled test (Test SS) contains a symmetric layout with two adjacent single-leaf panels with $2{,}820 \times 1{,}570$ mm^2 in-plane dimensions and 90 mm thickness. Conversely, a nonsymmetric specimen is considered in the second test (Test GO) with a solid right panel featuring a 20 mm gap between the wall and the flange of the top beam and a left panel with a central 520×943 mm^2 window-type opening corresponding to 11% of the panel area (see sketch in Fig. 3). The opening in the right panel was topped by a reinforced concrete lintel with a 130×90 mm^2 cross section. In both tests, the masonry panels were assembled using the same brick-units ($250 \times 90 \times 55$ mm^3) and 10 mm bed and 15 mm thick mortar joints. The panels were laid in contact with the beams and columns (except for the prescribed gap in the GO specimen) by casting a 10 mm mortar layer between frame and infill. The material properties obtained for the URM components in both infill tests (SS and GO) are presented in Table 2.

In order to induce the pushdown deformation, vertical hydraulic actuators were placed on the top of the central column and restrained by the reaction frame [Fig. 5(a)]. The restrained central column is allowed to translate vertically by means of sliding connector as shown in Fig. 5(b).

An initial test was carried out considering the bare frame with no masonry infill to determine its pushdown response. After the completion of the bare frame test, the angle cleats of the connections that were damaged were replaced before erecting the solid URM panels for the subsequent test. The physical behavior of the frame specimens was analyzed considering the experimental data provided by a combination of strain gauges and displacement transducers distributed at target locations on the specimens. A full description of the instrumentation layout can be found in Xavier (2015), whereas in this paper reference to instruments is made only when necessary for the sake of brevity.

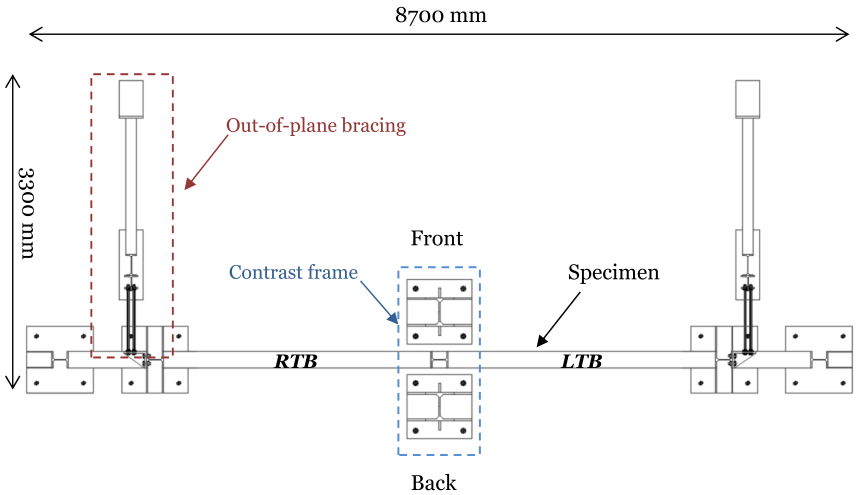

Fig. 4. Plan view of the experimental apparatus

Table 2. Material Properties for Specimens SS and GO

Test	Mortar compression $f_{c,m}$ (MPa)	Mortar tension $f_{t,m}$ (MPa)	Brick compression $f_{c,b}$ (MPa)	Brick tension $f_{t,b}$ (MPa)	Masonry compression $f_{c,M}$ (MPa)
SS	7.9	1.3	18.3	4.2	15.9
GO	13.9	—	18.3	4.2	—

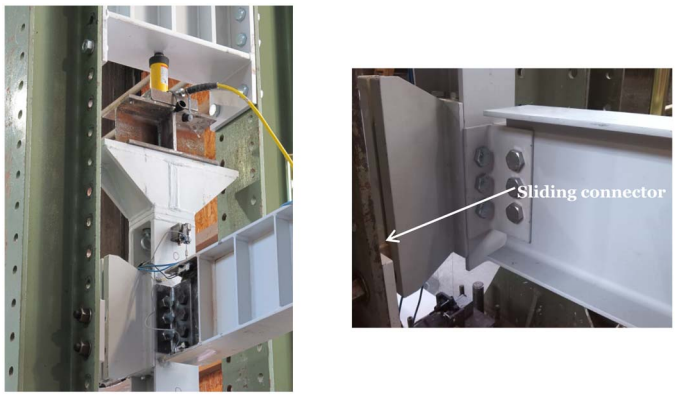

Fig. 5. Details of the testing apparatus: (a) reaction frame with a hydraulic actuator; (b) beam-column connection and central out-of-plane restraint system

Experimental Results

Bearing in mind the objectives stated in the "Introduction," the presentation of the results of the experimental campaign is made in two parts. In the first part, the pushdown capacity is evaluated by focusing primarily on the vertical force-displacement curves, which determine collapse resistance and energy absorption. In the second part, the detailed response of the two infilled cases (SS and GO) is evaluated, focusing on identifying the cracking and failure modes displayed by the URM panels during the deformation process.

Global Pushdown Response

The plots in Fig. 6 present the vertical load-displacement curves for the specimens under a quasi-static loading regime, where the vertical displacements are measured at the bottom of the central column. A first remark relates to the bare frame case (BF), where the response shown in Fig. 6 confirms that the structural system effectively behaves as a quasi-mechanism with negligible vertical resistance. Conversely, considering the infilled cases (SS and GO), it is evident that a high level of ductility is achieved, which primarily arises from the beam-column connection characteristics and the ductile behavior of confined infill masonry. The T-stubs (i.e., the assemblage of the connection components at each bolt row level) of the bolted connections allowed for considerable ductility under a tensile regime, but the small distance between the external bolt rows led to a reduced bending stiffness and strength. In addition to significant ductility in the pushdown response of the infilled frames, a remarkable vertical load capacity is observed. These two response characteristics guarantee significant energy absorption, which is a key factor for the resistance to progressive collapse. As discussed in the next section, this response is accompanied by extensive cracking in the masonry panels (in both Tests SS and GO). This confirms that despite the significant damage in the unreinforced walls, the confinement provided by the frame components led to a de facto frame-infill composite behavior as anticipated in the "Introduction." Furthermore, the overall stability of the panels was maintained to the end of the tests, even though the URM walls were characterized by considerably small thickness (90 mm). Interestingly, despite the differences in the infill configuration between Specimens SS and GO, a similar capacity was achieved toward the later stages of deformation. This is believed to be indicative of a progressive transfer of forces between the infill and the frame components. It develops when damage propagates in URM infill and prevents the degradation of the overall pushdown capacity even for very large vertical displacements at the central column. Finally, with respect to the masonry infill contribution to progressive collapse arrest, it should be pointed out that even though substantial damage developed in the masonry infill, as detailed in the next section, the global stability of the slender unreinforced panels was maintained during the whole range of pushdown displacements. The significant outcome is a monotonic increase of the energy absorption noticeable from the force-displacement curves (SS and GO) in Fig. 6.

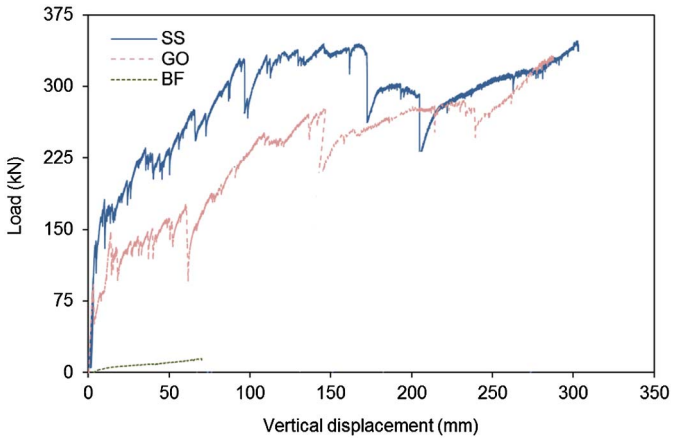

Fig. 6. Load-displacement pushdown response for Tests BF, SS, and GO

Detailed Response of URM Panels

Infilled Solid Symmetric Test—SS

Overall, the response of the solid infilled frame followed a displacement history quite similar to that experienced in lateral pushover tests. In particular, it was observed that stepped cracking developed along the compressed diagonal, eventually resulting in severe crushing and spalling at the compressed corners. Also extensive frame-infill separation in the tensile region was noticed.

The specimen response was characterized by an initial stage where nearly imperceptible cracks coalesced in the masonry panels, and frame-infill separation initiated. As the vertical force was increased, a continuous coalescence and propagation of horizontal and diagonal stepped cracks eventually branching into multiple diagonal cracks were observed. This is reflected in a highly stepped shape of the force-displacement curve until the maximum capacity is achieved (see SS curve in Fig. 6). A view of this crack pattern in the left panel is shown in Fig. 7(a). At this stage cracks propagate essentially through head and bed mortar joints; at later stages some of these initial cracks extended through brick units. Similarly a remarkable widening of crack widths occurred under increasing vertical displacement as shown in Fig. 7(b). As expected from the analogy with lateral pushover response, the onset of crushing in the compressive corners was observed together with fracture at the

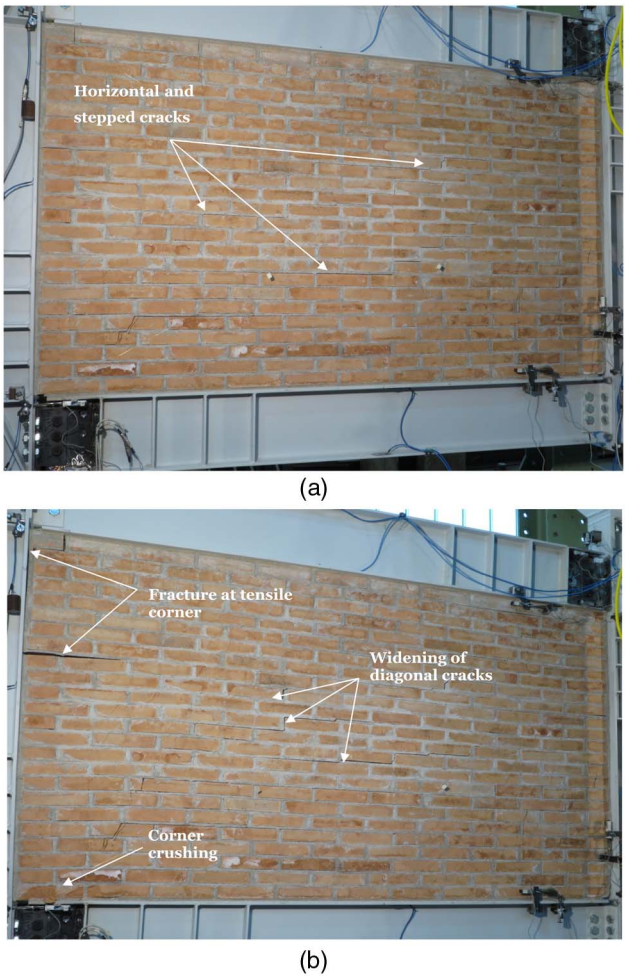

Fig. 7. Crack pattern in the left panel at (a) 20 mm; (b) 150 mm vertical displacement

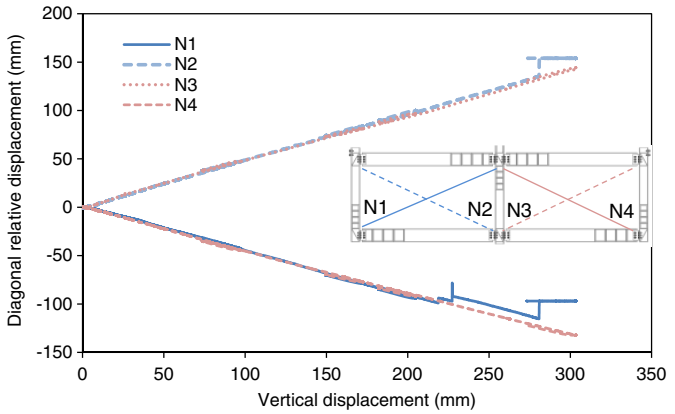

Fig. 8. Deformation of panels' diagonals (Test SS)

tensile zones. In particular, at the top-left corner of the left panel [tensile corner in Fig. 7(b)] a significant separation at the frame-infill interface was noticed and the rotation imposed to the top part of panel by the interaction with the confining structural elements caused the widening of horizontal cracks to accommodate such imposed deformation [Fig. 7(b)]. Overall, the left and right panels presented a similar damage pattern, but the evolution of cracks was not synchronized or symmetric, as a result of the inherent random distribution of mechanical characteristics and defects in masonry assemblages. In fact, even in physical tests on bare steel symmetric structures subjected to incremental pushdown, a deviation from a symmetric response is also observed, especially following the onset of damage at the connections.

Interestingly, regardless of the nonsynchronized crack evolution in the masonry panels, the infilled frame specimen presented a symmetric response, as the differential damage evolution in the two panels was accommodated by the surrounding steel frame. This is confirmed by the nearly identical variation of the diagonal deformations on the front face of the panels plotted in Fig. 8. These were measured by two transducers attached to the steel columns as sketched in Fig. 8. The eventual perturbations in the response at large displacements of the left part of the frame were caused by a series of detachments of masonry parts that impacted the diagonal instruments.

It is important to emphasize that the substantial deformation of the frame was allowed by large local rotations associated with plastic damage at the beam-column joints. The magnitude of the local deformations at the flexible bolted connections is analyzed in Figs. 9(a and b), where relative displacements at the connections are plotted against the vertical displacement at the bottom of the central column. In both cases a picture of the actual deformed pattern is presented for illustrative purposes. In the figures, a positive displacement value refers to a separation between beam's flange and column. These results clearly indicate significant rotations at the joints with a considerable stretching of the T-stubs. In Fig. 9(a), the sudden drop of the displacements measured by the transducer attached to the top flange is due to the malfunctioning of the instrument for vertical displacements exceeding 230 mm.

Another essential feature that was investigated regards the evolution of the frame-infill separation. Inspection of the crack pattern [Fig. 7(b)] indicates an effective compressive strut forms in the panel, transferring the vertical load to the lateral supports. For this to occur, a separation between the frame and infill has to develop in the opposite corners. This is visible in Fig. 10(a) at the central column-right bottom beam corner, and in Fig. 10(b) at the left column-left top beam area. In these pictures it is shown that a pronounced separation occurs at the interface between the panels and the columns, where the fracture is clearly localized along the frame-infill interface maintaining the adjacent mortar layer practically intact. Although relevant, this behavioral characteristic may be attributable to the generally weak mechanical characteristics of the physical interface between mortar layers and steel components. Note that as opposed to the infill-column interface, no separation is evident at the beam-infill interface. This is a consequence of the high stiffness of the beams composing the frame, which do not deform extensively in bending because of frame-infill interaction.

The variation of the relative displacements between the frame and the infill at the left bottom beam-central column tensile corner in presented in Fig. 11, where the total separation is given by

$$\Delta_{\text{Total}} = \sqrt{\Delta^2_{\text{Opening}} + \Delta^2_{\text{Sliding}}} \tag{2}$$

where Δ_{Total} = total separation; Δ_{Opening} = normal component; and Δ_{Sliding} = shear separation. The initial interface response is governed by the relative sliding between the column and infill, but an increasing dominance of the normal opening mode is observed at large displacements. Importantly, these measurements indicate that frame-infill separation is essentially a mixed mode problem as far as the nature of fracture is concerned.

To conclude the discussion on the experimental response of Specimen SS, a general view of the two panels in the final stages

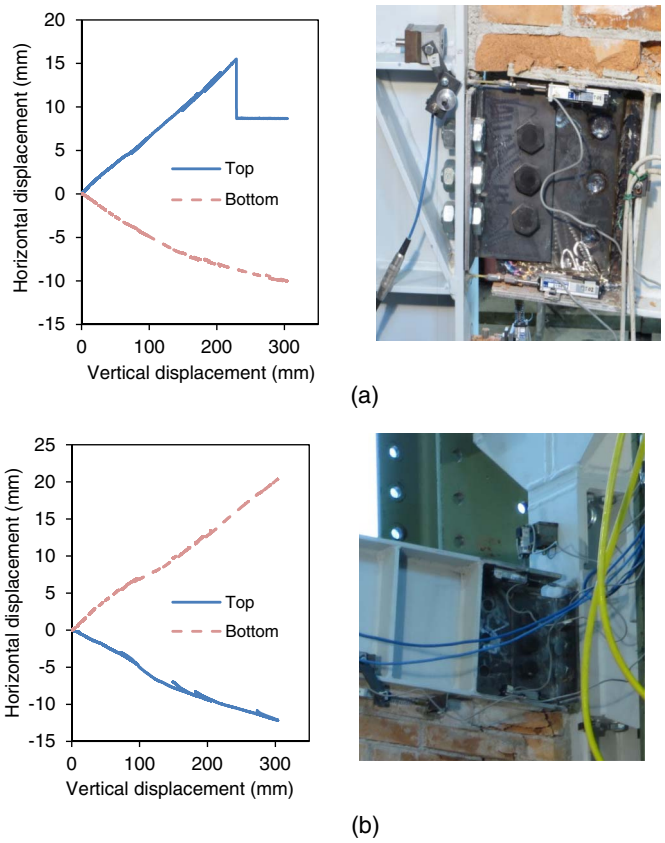

Fig. 9. Local deformations at connections between (a) LBB and LC; (b) LTB and CC [see Fig. 2(a) for members' location]

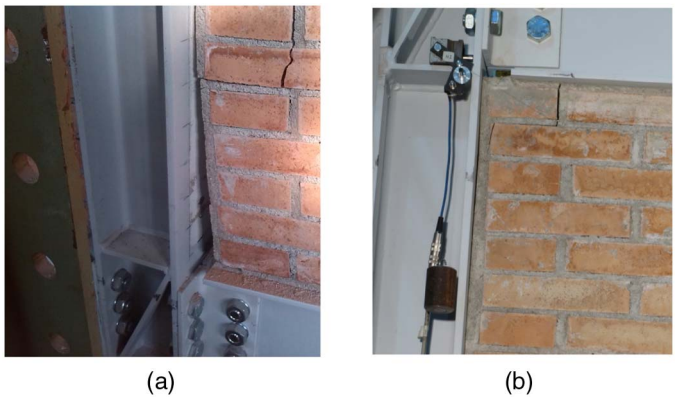

Fig. 10. Frame-infill separation: (a) CC-RBB; (b) LC-LTB corner (Test SS)

of the pushdown displacement is sketched in Fig. 12(a). This clearly shows the typical damage patterns associated with a strut idealization for the confined infill in both panels, including the stepped cracks along the diagonal direction and the crushing of the corners in compression.

Inspection of the damage in the panels, with the removal of the masonry parts that were practically detached from the load bearing walls, confirmed the full extent of the through thickness cracks in the brick-units [Fig. 12(b)]. This highlights the triaxial nature of the failure mode of masonry assemblages subjected to high compressive forces.

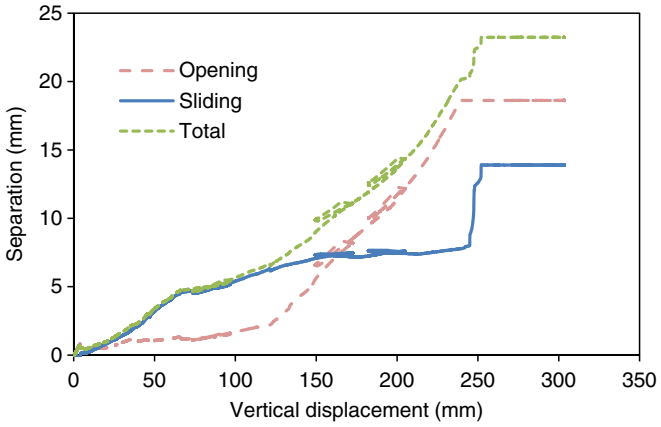

Fig. 11. Separation between left panel and bottom of central column (Test SS)

Infilled Test with Gap and Opening—GO

For the test of the infilled frame with gap and opening, following the initial cracking propagating from the corners of the opening in the right panel, damage developed in both panels. It is interesting to compare the global response of Specimen GO against that obtained in Test SS, as presented in Fig. 6. In particular, the two pushdown curves display similar trends. In general, the vertical forces measured in the test on Specimen GO are lower in the early and intermediate deformation stages. As the URM walls are extensively damaged and internal forces in steel frame members increase, the response of specimens SS and GO are characterized by approximately the same vertical force for the same vertical displacement. Of course, these observations are related to the particular relative stiffness and opening relative dimensions in the tested specimens.

Fig. 13 shows the variation of the relative displacements measured along the diagonal directions on the front face of the two panels. In particular, the displacement values obtained in this test are compared with those found in the test with solid panels (SS). The diagonal relative displacements in the two tests are practically coincident, confirming that the global frame response is symmetric also in the second test. This finding is particularly important, as it highlights that also in the case of nonsymmetric distribution of masonry infill, which is typically found in peripheral frames of realistic multistory buildings, the confinement effect provided by the frame to the URM panels leads to a symmetric deformation profile for adjacent frame bays. Of course, this observation has practical implication within the progressive collapse assessment framework mentioned in the "Introduction," as its underlying principle is the activation of a dominant pushdown mode. In this way, such a pushdown mode could still be valid for initially nonsymmetrical layouts provided there is a structural frame stiff enough to accommodate the differential internal response of the URM panels. Nevertheless, these considerations are for structural systems with flexible connections, where the frame deformations are mainly lumped at the joint locations. Extrapolation of this behavior to other structural typologies, as well as irregular spans, would require careful examination.

The local joint deformations are shown in Fig. 14, where the relative horizontal displacements between the beam flanges and the adjacent column are plotted against the vertical displacement at the bottom of the central column. Observing these experimental measurements it can be concluded that despite the nonsymmetrical configuration the joint response is fairly symmetrical. Moreover, it is important to stress that significant levels of joint deformation were achieved, which reinforces the key requirement of joint ductility to ensure the necessary levels of pushdown deformation.

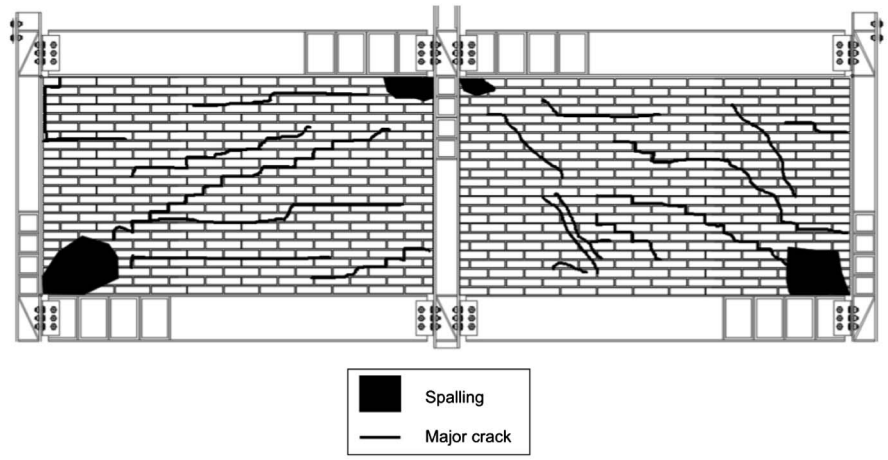

Fig. 12. (a) Survey of the final damage pattern of SS specimen; (b) detail of through thickness damage in the bottom compressed corners

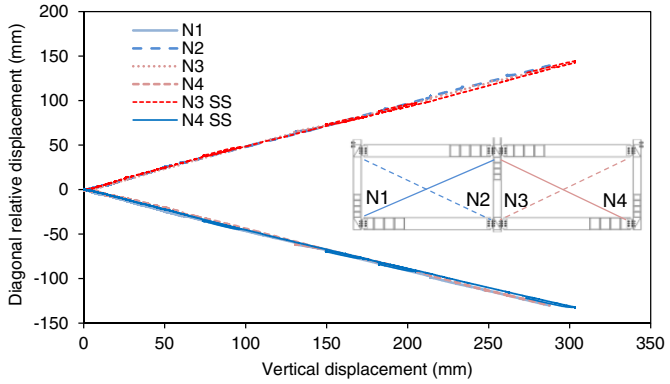

Fig. 13. Deformation of panel diagonals (Test GO)

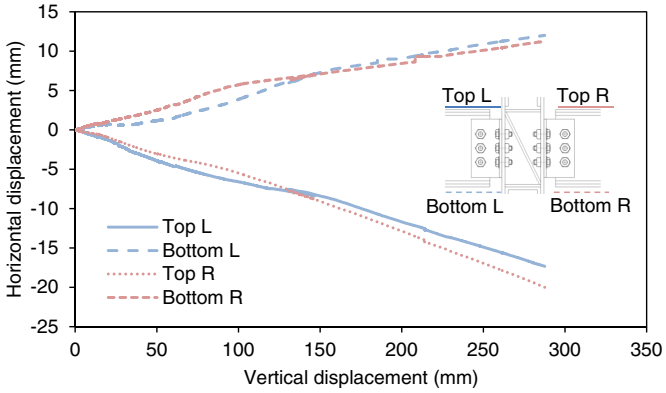

Fig. 14. Local deformations at the connections between the top beams and the central column (GO)

A noteworthy difference in comparison to the SS case regards the recorded evolution of frame-infill separation at the central column-left panel interface. As opposed to the results in Fig. 11, in the current case a predominantly sliding separation occurs. The recorded separation is given in Fig. 15(a), where the total separation is computed according to Eq. (2). This dissimilar behavior reflects the different responses of the two left panels in the SS and GO tests as the frames deform downward. This underlines the importance of the frame-infill interaction at their physical interface in controlling the forces transmitted between these components. Visual details of the frame-infill interaction are presented in Figs. 15(b and c), where the partial closure of the initial gap with the top beam and the initial separation at the bottom tensile corner of the left masonry panel are shown. Moreover, it is observed that a separation is maintained in the tension dominated region throughout the pushdown procedure.

Refocusing on the primary objective of the experimental program, inspection of the damage pattern in the perforated and solid (with gap) panels is performed in order to investigate its equivalence with the response expected from a lateral pushover test. With regards to the solid left panel, it is observed that an initial strut mechanism formed from the central column to the opposite compressed corner, even before the initial gap was closed. As the incremental downward deformation progressed after the initial gap was partially closed, a diagonal crack pattern similar to that in Test

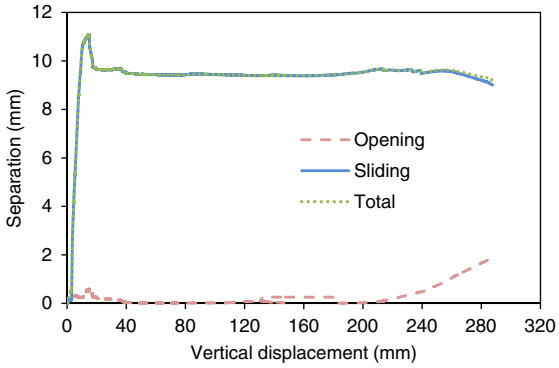

(a)

(b) (c)

Fig. 15. (a) Separation between left (solid) panel and bottom of central column (Test GO); (b) partial closure of initial gap; (c) separation at tensile corner

SS was also observed in the left solid wall, which confirms a compressive strut mechanism. At this stage, cracks mainly run along the mortar joints. Finally, toward the final phase of the pushdown process, the solid left panel displayed the typical damage modes expected from a lateral pushover test, with crushing in the compressed corner. A close-up inspection of the final damage in this panel is presented in Fig. 16. The crushing at the bottom corner confirms that masonry infill transferred the vertical force to the lateral supports through a compressive action along the diagonal direction. Similarly, the crack pattern in the top tensile region indicates the severity of the permanent damage imposed on the masonry wall, yet maintaining global stability. The remarkable nearly-vertical crack shown in Fig. 16(b) reflects the particular manner the load was transferred from the frame to the infill, which differs from that in the previous case (SS) as a result of the initial gap (implying an eccentric strut due to vertical friction between masonry and column).

Attention is now devoted to the response of the right panel, which has a central opening. Also in this case, an analogy with the behavior typically observed in infilled panels under horizontal forces can be established. The cracks shown in Fig. 17 developed from the corner of the window-type opening at the early stages of pushdown deformation. Subsequently, a new major crack coalesced and propagated from the top right corner of the opening eventually

(a) (b)

Fig. 16. Details of final damage in the left panel: (a) compressed area; (b) tensile area

Fig. 17. Final damage pattern in the right side panel: (a) right of the opening; (b) left of the opening

joining the initial crack in the panel's bottom compressed corner area leading to a major diagonal crack [Fig. 17(a)]. Simultaneously, cracks formed and propagated on the left region of the perforated panel [Fig. 17(b)], where a group of stepped cracks formed primarily along the mortar joints, running from the central column to the bottom beam. In Fig. 17(b), horizontal shear sliding along the bed joint at the level of the bottom part of the window can be also observed. Such sliding led to the fracture of the frame-infill interface at midheight of the central column. The propagation of damage in the perforated panel mainly corresponds to the widening of the cracks already described, until crushing of the compressed corners developed towards the final stages of the pushdown test. Nonetheless, stability of the masonry wall was maintained and no out-of-plane deformations were noticed. A survey of the damage pattern observed in the GO test is sketched in Fig. 18.

To conclude, the experimental results indicate that the failure mechanisms of confined URM panels subjected to pushdown deformations are similar to those typically found in masonry infill under lateral forces (typically referred to as pushover deformations). In particular, clear diagonal stepped cracks developed in all tests, which is in accordance with the common observation that diagonal cracking typically occurs in infilled frames composed of weak joints (El-Dakhakhni et al. 2003). Nonetheless, diagonal cracking did not lead to the failure of the panels, as the confinement provided by the steel frame allowed the masonry infill to accommodate such cracks and maintain a substantial load-carrying capacity for large pushdown displacements until corner crushing developed.

Energy-Based Interpretation of Experimental Pushdown Response

The tests reported earlier provided the necessary information to quantify the static pushdown capacity of confined URM infill panels. Nevertheless, as mentioned in "Ductility-Centered Robustness Assessment Framework," this is not sufficient to infer the progressive collapse mitigation potential of structural systems (Izzuddin et al. 2008). In fact, substantial experimental works available in the literature (for a wide range of structural systems and materials) fail to extrapolate the static pushdown results into meaningful progressive collapse resistance metrics. Toward this end, the pushdown responses obtained in the SS and GO tests are investigated within the scope of the progressive collapse assessment framework briefly described in "Ductility-Centered Robustness Assessment Framework." In particular, the experimental nonlinear static curves in Fig. 6 are transformed into pseudostatic responses [according to Fig. 1(b)], leading to the results depicted in Fig. 19. This pseudostatic capacity represents the actual collapse resistance of the affected structure, providing a singular measure accounting for strength, redundancy, energy absorption, and

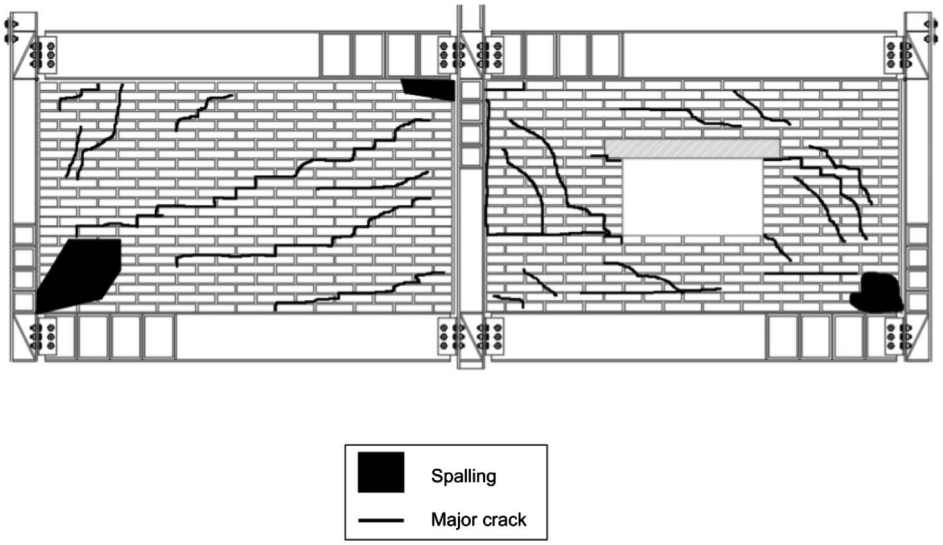

Fig. 18. Survey of the final damage pattern of GO specimen

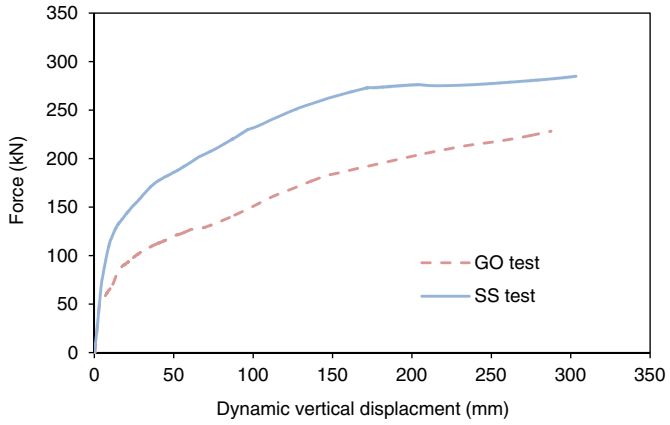

Fig. 19. Pseudostatic curves for the infilled tests

dynamic effects (Izzuddin et al. 2008). A noteworthy finding arises from a comparative assessment of the nonlinear static (Fig. 6) and pseudostatic (Fig. 19) curves. While in the former, both SS and GO capacities converge to the same value toward the end of the pushdown test, inspection of the pseudostatic curves clearly indicates that the collapse resistance of specimen SS is actually substantially higher than the GO counterpart. Such a difference in robustness enhancement is principally governed by increased energy absorption when solid panels are used. Furthermore, an energy-based interpretation of the tests, following the procedure depicted in Fig. 1, constitutes a fundamental aspect in a realistic appraisal of the progressive collapse potential of structural systems, as merely inspecting the static pushdown capacity might lead to erroneous conclusions. With regard to this aspect, it is known that typical engineering assessments are based on force (or stress) checks for a given target displacement (ductility) level. However, what the comparison considering the two infilled specimens emphasizes is that such an approach is inadequate for robustness assessment, meaning that a proper account of energy absorbed up to a given displacement must be considered in relation to the energy imparted by the suddenly applied load. Also, according to Izzuddin et al. (2008), the pseudostatic capacity of the peripheral infilled frames can be conveniently added to that of other members such as transverse beams and floor slabs, allowing a rational assessment of the relative importance of the activated mechanism. This is important, for instance, when deciding which members to enhance in terms of strength and ductility for effective robustness design (or retrofit).

In order to conclude the energy interpretation of the test, a strut-based model is employed to complement the analysis of the experimental results. The three-strut model proposed in El-Dakhakhni et al. (2003) is adopted as representative of the multistrut procedures available in the literature. Opting for a multistrut instead of a single-strut model arises from the experimental observations that the evolution of frame-infill interaction is too complex to be captured by a single strut representation. A sketch of the simplified model is shown in Fig. 20(a), where the area of the strut is given as (El-Dakhakhni et al. 2003)

$$A = \frac{(1-\alpha_c)\alpha_c h t}{\cos\theta} \tag{3}$$

where $t = 90$ mm is the thickness of the masonry panels, with the necessary input parameters listed in Table 3; more details on the model can be found in Xavier (2015). Because of the simplified nature of strut idealizations, only the solid SS test is addressed in this paper in order to circumvent the uncertainty associated with strut modeling of URM panels with gaps and openings.

Before proceeding with the simplified analysis, a proper calibration of the bare frame model is needed. In particular, the adopted type of beam-column connection poses a substantial challenge because its mechanical behavior is difficult to quantify according to

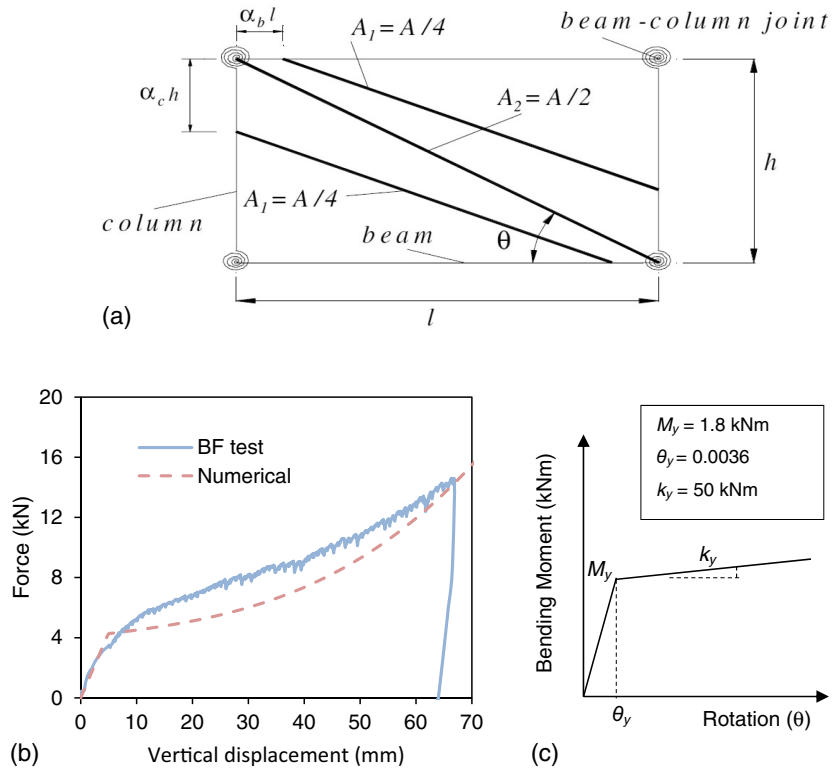

Fig. 20. (a) Three-strut model proposed by El-Dakhakhni et al. (2003); (b) calibration of the steel frame FE model; (c) rotational spring model

Table 3. Geometrical and Material Properties for the Strut Model (Test SS)

Parameter	Value
α_c	0.4
α_b	0.4
A (mm^2)	5,1923
f_c (MPa)	7.95
ε_{cr}	0.01

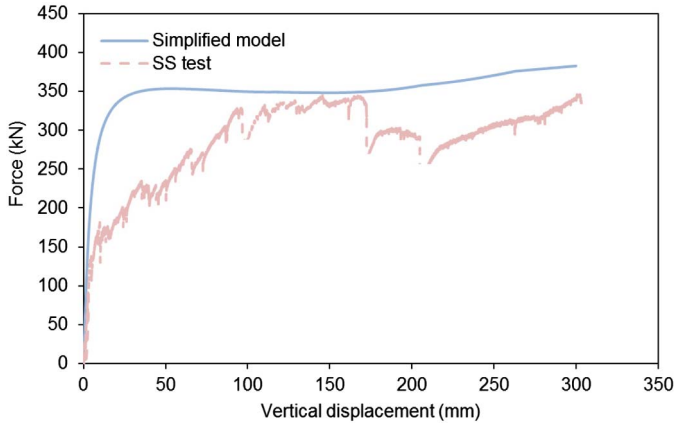

Fig. 21. Comparison between SS test and simplified numerical model

current design guidelines. The flexible bolted joints with clearance holes were designed to provide significant axial and shear strength to accommodate the forces arising from frame-infill interaction, while displaying reduced bending strength and stiffness. In the adopted frame description, a rotational spring with a simplified bilinear moment-rotation constitutive curve is employed to represent the flexural characteristics of the joint. The stiffness and resistance parameters for the nonlinear spring were calibrated to obtain an accurate response prediction of the bare frame subjected to pushdown displacements as shown in Fig. 20(b).

A comparison between the pushdown curves computed with the simplified model and that obtained in test SS is plotted in the graph of Fig. 21. Overall, the numerical prediction represents an envelope of the experimental response. Clearly the initial branch of the pushdown curve computed with the simplified model overpredicts the real capacity, whereas as the peak resistance is approached, a better match with experimental values is achieved. This is explained by the inherent inability of the utilized simplified model to capture the actual damage evolution in the panels which comprises an initial stage with formation and propagation of diagonal cracks followed by the crushing at the compressed corner. The latter event limits the maximum vertical resistance. Conversely, the considered simplified model accounts for the crushing mode but does not represent the progressive degradation of stiffness due to the evolution of cracks within the panels. For this reason, only the maximum capacity is fairly estimated. The pseudostatic curve related to the simplified model of Test SS is contrasted to that of the real test in Fig. 22. The reason for this comparison is to raise awareness to the fact that even though the nonlinear static response from the simplified model could be regarded as acceptable for design-purposes, especially for the large displacement domain (Fig. 21), when the energy-based robustness assessment framework is employed a more pronounced discrepancy is evident. This emphasizes that the considered simplified modeling approach is inadequate for progressive collapse assessment under sudden column loss because this requires a proper account of energy absorbed up to a specific level of displacement.

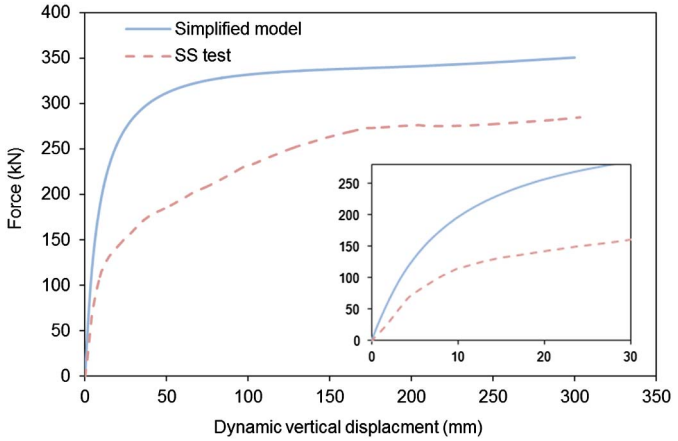

Fig. 22. Experimental and numerical pseudostatic capacity (Test SS)

A close-up view of the curve in Fig. 22 confirms that this discrepancy is also pronounced at the initial stage of pushdown displacement. This is particularly important because, according to the preliminary numerical results in Xavier et al. (2015), one of the primary advantages ensuing from due consideration of URM infill in robustness assessment is the potential to arrest collapse at small vertical displacements, avoiding the activation of other secondary mechanism such as floor membrane and beam catenary actions.

Summary and Conclusions

The results from real-scale experiments are reported in this paper, where the pushdown responses of two URM infilled frames are investigated within the scope of robustness assessment of framed building structures under single column loss. The experimental results provide evidence that the mechanical behavior of masonry infill panels subjected to incremental pushdown deformations exhibits the same features as expected from lateral pushover tests. In particular, the development of the so-called compressive strut mechanism is observed, effectively transferring the applied force at the central column to the lateral supports. Such a mechanism was highlighted by the appearance of diagonal stepped cracking at early stages of deformation, eventually leading to crushing of the compressed corners. Similarly, noticeable fracture and separation at the tensile frame-infill interface is evident.

The presented experimental results confirm the potential robustness reserve associated with URM infill confined by the structural frame, as often found in existing constructed facilities. Also noteworthy is that a stable resisting capacity is achieved, even when accompanied by extensive damage in the masonry panels, further underlining the importance of frame-infill interaction. In this respect, it is shown that a considerable pushdown capacity is sustained even at large displacements. Nevertheless, the role of the joint ductility in accommodating this level of deformation must be given due consideration.

Two typologies of masonry infill were tested: (1) a simple solid symmetry case, and (2) a nonsymmetrical layout including a solid wall with a gap between the frame and infill and a perforated panel. Both cases provided significant pushdown capacity, showing that even walls with gaps and openings, as commonly used in exterior building cladding, can significantly increase robustness under column loss. Despite the results obtained considered relatively thin URM walls, additional experimental research is required to investigate the response of very slender panels, where the confining effects provided by the frame to masonry infill may potentially cause

out-of-plane instability of the masonry components associated with substantial degradation of pushdown resistance. Finally, careful interpretation of the static resistance is necessary for inferring progressive collapse resistance. In this respect, the experimental results are considered within the robustness assessment framework developed by Izzuddin et al. (2008). Such analysis reveals that despite similar static capacities at large displacement, the higher energy absorbed in the SS specimen leads to a significant enhancement in the contribution to robustness under sudden column loss. Simplified numerical simulations with practical descriptions for the infill specimen featuring solid URM panels were carried out, considering the energy-based robustness assessment framework to investigate progressive collapse resistance. Notable discrepancies with the results based on the physical tests were found confirming that, for realistic robustness assessments, numerical descriptions capable of accurately representing the actual response at different levels of pushdown deformations should be employed.

This experimental program provided mechanically sound and quantifiable evidence that nonstructural masonry infill panels in peripheral frames constitute a reliable and efficient source of enhanced robustness under column loss events.

Acknowledgments

The authors acknowledge the support provided by the Portuguese Foundation for Science and Technology (FCT) through the doctoral grant SFRH/BD/70935/2010 to the first author. The authors also acknowledge Dr. Franco Trevisan for his assistance during the construction of the specimens, execution of the tests, and data collection.

References

Adaros, M., and Smilowitz, R. (2014). "Challenges and considerations for the retrofit of existing structures for progressive collapse." *J. Perform. Constr. Facil.*, 29(5), B4014001-1–B4014001-9.

Arup (2011). *Review of international research on structural robustness and disproportionate collapse*, Dept. for Communities and Local Government, DCLG Publications, London.

CEN (European Committee for Standardization). (2006). "Actions on structures. Part 1–7: General actions—Accidental actions." *Eurocode 1 EN 1991-1-7*, Brussels, Belgium.

Cormie, D., Mays, G., and Smith, P., (2009). *Blast effects on buildings*, Thomas Telford Publishers, London.

El-Dakhakhni, W., Elgaaly, M., and Hamid, A. (2003). "Three-strut model for concrete masonry-infilled steel frames." *J. Struct. Eng.*, 10.1061/(ASCE)0733-9445(2003)129:2(177), 177–185.

Farazman, S., Izzuddin, B. A., and Cormie, D. (2013). "Influence of unreinforced masonry infill panels on the robustness of multi-storey buildings." *J. Perform. Constr. Facil.*, 10.1061/(ASCE)CF.1943-5509.0000392, 673–682.

Izzuddin, B. A. (2010). "Robustness by design—Simplified progressive collapse assessment of building structures." *Stahlbau*, 79(8), 556–564.

Izzuddin, B. A., and Nethercot, D. A. (2009). "Design-oriented approaches for progressive collapse assessment: Load-factor vs ductility-centered methods." *Structures 2009: Don't Mess with Structural Engineers*, ASCE, Reston, VA, 1791–1800.

Izzuddin, B. A., Vlassis, A. G., Elghaz1ouli, A. Y., and Nethercot, D. A. (2008). "Progressive collapse of multi-storey buildings due to sudden column loss—Part I: Simplified assessment framework." *Eng. Struct.*, 30(5), 1308–1318.

Li, B., and Qian, K. (2014). "Are the frail designed to fail? Assessing the collapse risk of existing structures." *Structures Congress 2015*, ASCE, Reston, VA.

Mosalam, K. M., and Gunay, S. (2015). "Progressive collapse of reinforced concrete frames with unrienforced masonry infill walls considering in-plane/out-of-plane interaction." *Earthq. Spec.*, 31(2), 921–943.

Naderi, D., Adaros, M., and Wood, S. (2015). "Use of ring beams for progressive collapse retrofit." *Structures Congress 2015*, ASCE, Reston, VA.

Negro, P., and Colombo, A. (1997). "Irregularities induced by nonstructural masonry panels in framed buildings." *Eng. Struct.*, 19(7), 576–585.

Smith, P. P., Byfield, M. P., and Goode, D. J. (2010). "Building robustness research during World War II." *J. Perform. Constr. Facil.*, 10.1061/(ASCE)CF.1943-5509.0000115, 529–535.

Vlassis, A. G., Izzuddin, B. A., Elghazouli, A. Y., and Nethercot, D. A. (2008). "Progressive collapse of multi-storey buildings due to sudden column loss—Part II: Application." *Eng. Struct.*, 30(5), 1424–1438.

Xavier, F. B. (2015). "The role of masonry infill in progressive collapse mitigation of multi-storey buildings." Ph.D. thesis, Dept. of Civil and Environmental Engineering, Imperial College London, London.

Xavier, F. B., Macorini, L., and Izzuddin, B. A. (2015). "Robustness of multistory buildings with masonry infill." *J. Perform. Constr. Facil.*, 10.1061/(ASCE)CF.1943-5509.0000684, B4014004-1–B4014004-12.